

Oxygen-bonding environments in glow-discharge-deposited amorphous silicon-hydrogen alloy films

G. Lucovsky,* J. Yang, S. S. Chao, J. E. Tyler, and W. Czubytyj
Energy Conversion Devices, Inc., 1675 West Maple Road, Troy, Michigan 48084
(Received 17 March 1983)

This paper presents the results of a systematic study of oxygen incorporation in *a*-Si:H alloys produced by the glow-discharge decomposition of SiH₄, H₂, and O₂. We identify four oxygen-related absorption bands, at 2090, 980, 780, 500 cm⁻¹, and show that the absorption strength in each band scales linearly with the oxygen concentration. We demonstrate that oxygen can increase the solubility of hydrogen in *a*-Si in the monohydride bonding geometry. The features identified above are shown to be characteristic of a bonding site in which the oxygen and hydrogen atoms are bonded to the same silicon atom. We find no features in the infrared absorption that are associated with bonding configurations having OH groups. In films containing both oxygen and polysilane bonding, as evidenced by the doublet absorption at 845 and 890 cm⁻¹, we find no evidence for bonding sites in which a substantial fraction of the silicon atoms have one oxygen and two hydrogen neighbors.

I. INTRODUCTION

Thin films of hydrogenated amorphous silicon (*a*-Si:H) sometimes contain significant amounts of unintentionally added oxygen. This can either be detected via secondary-ion mass spectrometry (SIMS), or if the bonded-oxygen concentration exceeds about 0.5 at. %, it is readily detected by infrared (ir) absorption through the presence of a broad band at about 980 cm⁻¹.¹ Films have also been prepared in which oxygen is intentionally added as a third alloy constituent, *a*-Si:(H,O).¹⁻³ In films with hydrogen concentrations of about 5–15 at. % and oxygen concentrations of about 1–5 at. % there have been reports of three oxygen-related ir absorptions at approximately 2090, 980, and 780 cm⁻¹.^{2,4} It has been shown that all three features can be explained by the local vibrations of a configuration in which oxygen and hydrogen atoms are bonded to the same silicon atom.^{4,5} There is no evidence for the existence of OH groups. The absorption at 2090 cm⁻¹ is the Si–H bond-stretching vibration of a monohydride-bonding arrangement. Its frequency has been shifted from 2000 cm⁻¹ as in “pure” *a*-Si:H to 2090 cm⁻¹ by an induction effect associated with the oxygen atom being backbonded to the silicon atom.^{3,6} The vibration at 980 cm⁻¹ is the asymmetric stretching vibration of the oxygen atom in its twofold-coordinated bridging bonding site. Its frequency is also shifted by changes in the force constants associated with the near neighbor hydrogen atom, from 940 cm⁻¹ in *a*-Si:O⁷ to the value of 980 cm⁻¹ in the *a*-Si:(H,O) alloys. Finally the mode at 780 cm⁻¹ is a vibration which strongly couples Si–H and Si–O–Si motions.^{4,5} It is a vibration that is specifically determined by the detailed character of the bonding geometry. It occurs only when the Si–H bond is the same plane of the Si–O–Si bond, and when the oxygen and hydrogen atoms are in the *cis* bonding geometry (see Refs. 4 and 5 for details of the arguments that lead to this conclusion).

This paper presents a systematic study of oxygen incorporation in thin films of *a*-Si:(H,O) produced by glow-discharge decomposition of SiH₄ in an oxygen and hydro-

gen ambient. The deposition conditions have been adjusted to produce films with substantially all of the hydrogen in monohydride-bonding configurations. The oxygen concentration has then been varied over a relatively wide range and the ir absorption has been studied. In addition to the modes discussed above, we have identified a fourth vibration at 500 cm⁻¹ that also scales with the oxygen concentration. By comparison with the absorption bands in *a*-Si:O films,⁷ this is assigned to an out-of-plane rocking mode of the Si–O–Si group. Infrared absorption near 500 cm⁻¹ is also observed in a number of other alloy systems, e.g., *a*-Si:F. In many instances this absorption is related to the motion(s) of the Si atom (atoms) that is bonded to the alloy atom. The amount of ir activity then derives from the degree of charge transfer between the alloy atom and its immediate Si neighbors. In the case of O, the absorption at 500 cm⁻¹ in ion-implanted films is considerably stronger than in other alloys and the alternative explanation given above has been proposed.⁷ This is supported by comparisons with *a*-SiO₂, wherein the out-of-plane rocking motion of the oxygen atoms gives rise to a very strong ir absorption close to 475 cm⁻¹. We also find a synergistic effect between the amount of oxygen and the solubility of hydrogen in the monohydride-bonding geometry. For a given set of deposition parameters, and above an oxygen concentration of about 2 at. %, there is an increase in the hydrogen incorporation that is proportional to the oxygen concentration. This is additional experimental evidence for the strong association of oxygen and hydrogen atoms at a common silicon-bonding site.

We have also grown films in which the oxygen concentration has been held constant, but with the deposition conditions changed to yield hydrogen incorporation in the SiH₂ and (SiH₂)_n bonding configurations. The ir spectra of these films show characteristic polysilane absorption bands, but do not show additional features associated with oxygen atoms bonded to silicon sites containing more than one hydrogen. We have also studied the ir absorption in films with a constant hydrogen concentration, but greatly enhanced oxygen concentrations, in effect alloys to the

form $\alpha\text{-SiO}_{2-x}\text{H}_x$. We find two hydrogen-related features, a bond-stretching mode at 2250 cm^{-1} and a bond-bending mode at about 870 cm^{-1} . These are the vibrations expected from the symmetry of SiH site in an $\alpha\text{-SiO}_2$ host.

Section II presents the details of film preparation and the chemical analysis. Section III includes the ir absorption spectra and the results of our analysis of the absorption strength as a function of the oxygen concentration. Also included in this section are the spectra of films with the higher hydrogen and oxygen concentrations. Section IV is a discussion of the experimental data that draws heavily on the model calculations discussed in Refs. 4 and 5. Finally, Sec. V summarizes the important points made in the paper.

II. FILM PREPARATION AND CHARACTERIZATION

Thin-film samples of $\alpha\text{-Si}(\text{H},\text{O})$ were prepared by the glow-discharge decomposition of SiH_4 in a gas ambient containing both H_2 and O_2 . The ratio of $\text{SiH}_4\text{:H}_2$ was maintained at 1:1, and the oxygen concentration was varied between 5 and 2000 ppm. The deposition conditions for these runs were adjusted to produce films in which the hydrogen is incorporated predominantly in the SiH- (or monohydride-) bonding configuration. The glow-discharge chamber is a capacitively coupled system similar to that described by Knights.⁸ The particular deposition parameters were the following: (1) a substrate temperature of 300°C , (2) an input power of 10 W, and (3) a pressure of 0.5 Torr. Prior to each run the sample chamber was baked and pumped for a time sufficient to remove any residual water vapor which would have contributed to the oxygen content of the films. The conditions for this bakeout and pumpdown were established by producing films with no intentionally added oxygen, and then determining by ir if any oxygen was present. The procedure we used ensured that the residual oxygen concentration was well below ~ 0.2 at.%. Two films were grown at lower substrate temperatures, 50 and 100°C , respectively, in order to promote the incorporation of additional hydrogen in the polysilane bonding configuration. The amount of oxygen added to the gas flow in these two films was 500 ppm. In all of the films described above, the deposition parameters yielded films in which the hydrogen concentration was greater than or equal to the oxygen concentration. Finally, one film was grown under conditions that yielded an oxygen concentration well in excess of the incorporated hydrogen concentration, essentially hydrogen-"doped" $\alpha\text{-SiO}_2$. All of the films were deposited on high-resistivity crystalline-silicon substrates. The deposition time was set to give films of nominal thickness $1\ \mu\text{m}$. Actual thicknesses were measured using an interferometric technique.

The chemical composition of the films was obtained via electron-microprobe analysis and SIMS. The oxygen concentration was determined via the electron-microprobe technique. This in turn provides a way of calibrating the ir absorption data for the 980-cm^{-1} band, and thereby establishing the ir absorption as a secondary standard. If

$I(980\text{ cm}^{-1})$ is the integrated absorption (in units of eV cm^{-1}) in the 980-cm^{-1} band and $C(\text{O})$ is the oxygen concentration (units of at. %), then we find that

$$C(\text{O}) = A(\text{O})I(980\text{ cm}^{-1}), \quad (1)$$

where $A(\text{O}) = 0.156$ at. %/ eV cm^{-1} . The hydrogen concentration $C(\text{H})$ was measured by SIMS using Ar^+ ions as the sputtering source and H-ion-implanted samples as standards. The concentrations so obtained are in excellent agreement with concentrations determined from the integrated ir absorption in the 2000-cm^{-1} band, $I(2000\text{ cm}^{-1})$ using previously published proportionality constants.^{9,10} In particular, our SIMS results support the relationship given in Ref. 10,

$$C(\text{H}) = A(\text{H})I(2000\text{ cm}^{-1}), \quad (2)$$

where $A(\text{H}) = 0.77$ at. %/ eV cm^{-1} .

The films grown at 300°C show no evidence via scanning-electron-microscope (SEM) micrographs for any columnar growth morphology. In contrast, the films grown at both 50 and 100°C show clear evidence for columnar structure (see papers cited in Ref. 10).

III. EXPERIMENTAL RESULTS

The ir absorption spectra were recorded using a Perkin-Elmer model 580B double-beam recording spectrophotometer. The absorption spectrum was obtained by placing the thin-film sample (on a crystalline-silicon substrate) in one beam and a matched piece of crystalline silicon in the reference beam. Using this technique we obtain the differential absorption which is due to the thin film of $\alpha\text{-Si}(\text{H},\text{O})$. Spectra were run in the frequency regime between 400 and 4000 cm^{-1} with a resolution of approximately 3 cm^{-1} . The model 580B system is used with a microcomputer data-acquisition system, a Perkin-Elmer model 3600 data station. By running multiple scans and averaging we are able to obtain the transmission to better than $\pm 0.5\%$. The instrument is purged with dry nitrogen; however, as seen in the spectra shown in Figs. 1(a)–1(d), there is some residual water-vapor absorption in the region between 1200 and 1800 cm^{-1} . This occurs in a region of the spectrum that does not have any first-order vibrations associated with either the $\alpha\text{-Si}$ host or the oxygen and hydrogen alloy atoms.

Figure 1 shows spectra for the following four samples with increasing oxygen content: (a) 0.9 at. % oxygen, (b) 3.6 at. %, (c) 6.0 at. %, and (d) 12.7 at. %. The hydrogen concentration in these samples is approximately 15 at. %. We have indicated in the figure the positions of the SiH group bond-stretching and bond-bending absorptions, $\nu_S = 2000\text{ cm}^{-1}$ and $\nu_B = 630\text{ cm}^{-1}$, respectively, as well as the positions of the Si-O-Si group bond-stretching, bond-bending, and bond-rocking absorptions, $\nu'_S = 940$, $\nu'_B = 650$, and $\nu'_R = 500\text{ cm}^{-1}$. The atomic motions associated with these particular absorptions are discussed in the next section of this paper and are displayed in Fig. 10. The main point we wish to make with respect to the spec-

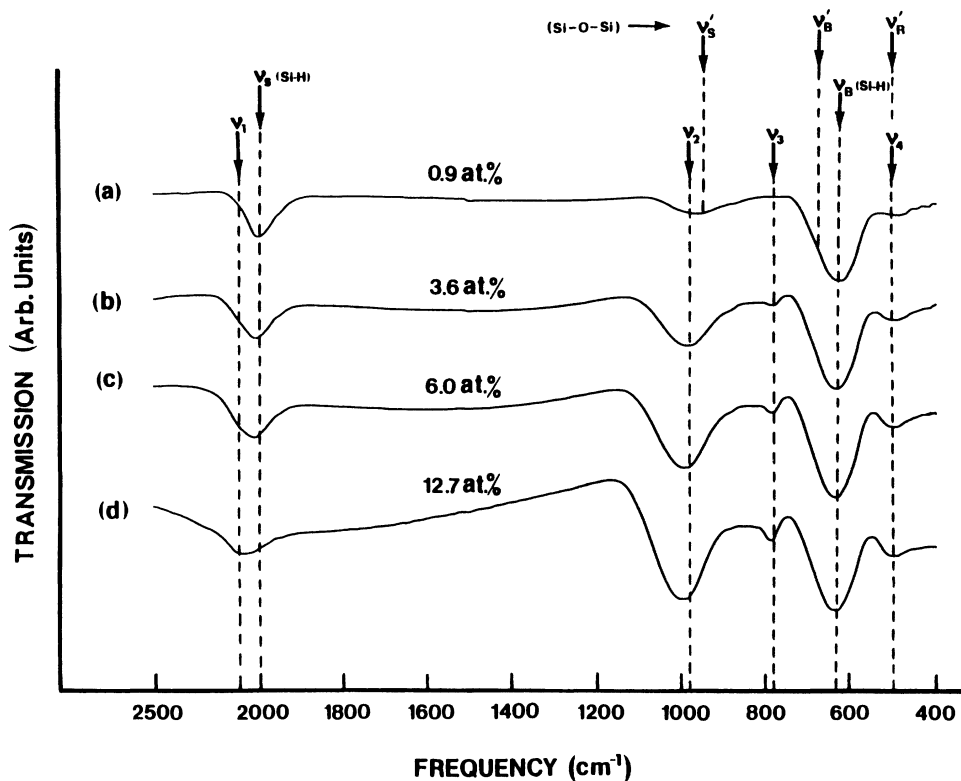


FIG. 1. Infrared transmission spectra of four *a*-Si:(H,O) alloy films with increasing oxygen concentrations: (a) 0.9 at. % oxygen, (b) 3.6 at. %, (c) 6.0 at. % and (d) 12.7 at. %. Arrows designated ν_S and ν_B indicate the frequencies of Si-H vibrations in *a*-Si:H, while the arrows designated ν'_S , ν'_B , and ν'_R indicate the frequencies of the Si-O-Si vibrations in *a*-Si:O. Arrows marked ν_1 , ν_2 , ν_3 , and ν_4 are the four oxygen-related features in the *a*-Si:(H,O) alloys.

tra displayed in Fig. 1 concerns the oxygen-related features that we have labeled ν_1 , ν_2 , ν_3 , and ν_4 . Note that ν_1 and ν_2 occur at frequencies which are shifted, respectively, from ν_S and ν'_S , so that they are not simply SiH and Si-O-Si bond-stretching vibrations associated with vibrationally isolated SiH and Si-O-Si centers. The vi-

bration we have labeled ν_3 appears to be unique to *a*-Si:(H,O) alloys, and as we shall discuss later is a coupled mode involving significant hydrogen and oxygen atomic displacements.^{4,5} Finally the fourth mode ν_4 occurs at very nearly the same frequency as the rocking mode ν'_R of an isolated Si-O-Si group. The features, ν_1 , ν_2 , ν_3 , and ν_4 all grow with increasing oxygen concentration. It is clear from the figure that the absorption spectra of *a*-Si:(H,O) alloys are not simply a linear superposition of SiH and Si-O-Si spectra. This in turn means that there

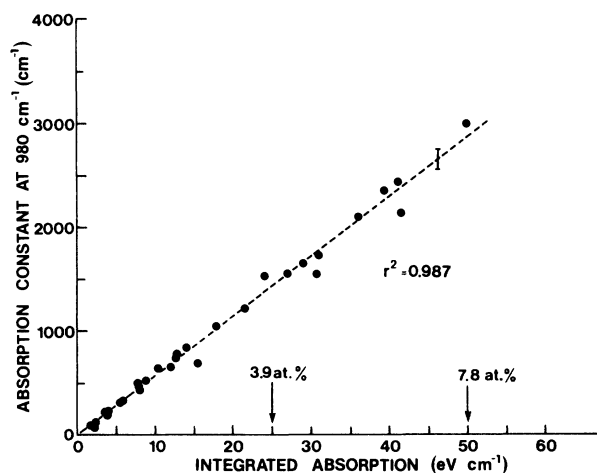


FIG. 2. Plot of the value of the absorption constant at 980 cm^{-1} as a function of the integrated absorption in the 980- cm^{-1} band. Dashed line is linear regression analysis of the ir data. Error bars shown on the plot as well as the r^2 value indicate the degree to which the data are represented by a linear relationship. Also shown on the figure are the oxygen concentrations corresponding to two values of the integrated absorption.

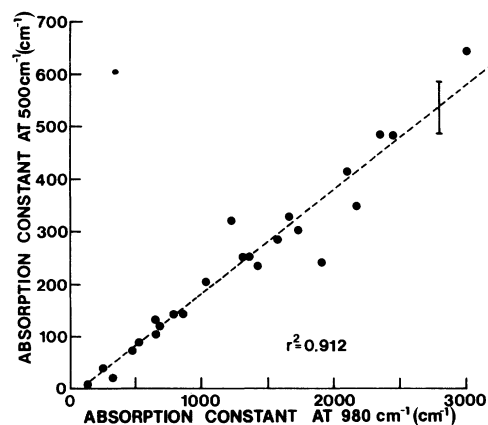


FIG. 3. Absorption constant at 500 cm^{-1} vs absorption constant at 980 cm^{-1} . Dashed line is a linear regression analysis of the data. Error bars shown in the diagram and the r^2 value indicate the quality of the linear fit.

are new local bonding arrangements in the alloys in which both hydrogen and oxygen atoms are bonded to the same or near-neighbor silicon atom sites. We will now demonstrate that all four oxygen related features display a linear scaling relationship with the amount of bonded oxygen.

We first consider the strongest oxygen related feature at 980 cm^{-1} , and in Fig. 2 we display a plot of the absorption constant at the position of the peak absorption versus the integrated absorption in the 980-cm^{-1} band. The dotted line shown in the figure is a linear regression analysis of the data. The r^2 value for this analysis is 0.987 indicating the validity of the linear relationship that holds for well over an order of magnitude of oxygen concentration. We have indicated in the diagram the oxygen concentrations for two values of the integrated absorption. The linearity between the value of the maximum absorption and the integrated absorption is a result of the line shape of the ir band remaining constant over the range of oxygen incorporation we have considered. At higher oxygen concentrations the maximum in the absorption shifts to higher energy and, for compositions approaching $\alpha\text{-SiO}_2$, the line shape changes with the development of a satellite feature at the high-frequency side of the band (see Fig. 3 of Ref. 11). Having established the equivalence between the integrated absorption in the 980-cm^{-1} band and the peak value of the absorption constant at 980 cm^{-1} , we now analyze the other three oxygen-related features and in particular we demonstrate that their intensities scale with that of the 980-cm^{-1} band.

Figures 3–5 display the values of the absorption constants at 500 cm^{-1} (ν_4 of Fig. 1), 780 cm^{-1} (ν_3 of Fig. 1), and 2090 cm^{-1} (ν_1 of Fig. 1) as a function of the absorption constant at 980 cm^{-1} (ν_2 of Fig. 1). All three sets of data have been subjected to a linear regression analysis. The r^2 values shown in the figures are all in excess of 0.9 indicating the validity of a linear relationship. The relatively small values of the absorption constants at 500 and 780 cm^{-1} introduce uncertainties into the data and thereby the analysis yields small offsets along the x axis. In

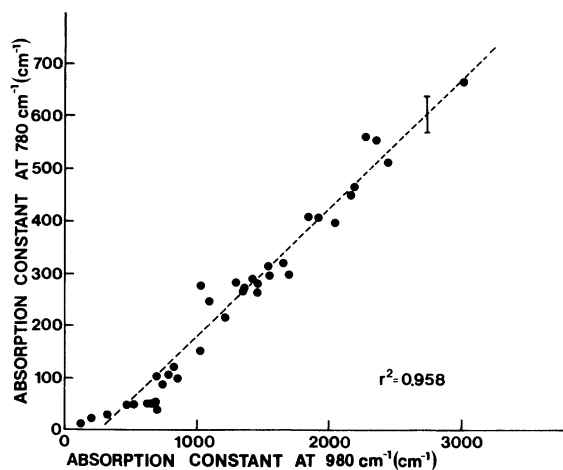


FIG. 4. Absorption constant at 780 cm^{-1} vs absorption constant at 980 cm^{-1} . Dashed line is a linear regression analysis of the data. Error bars shown in the diagram and the r^2 value indicate the quality of the linear fit.

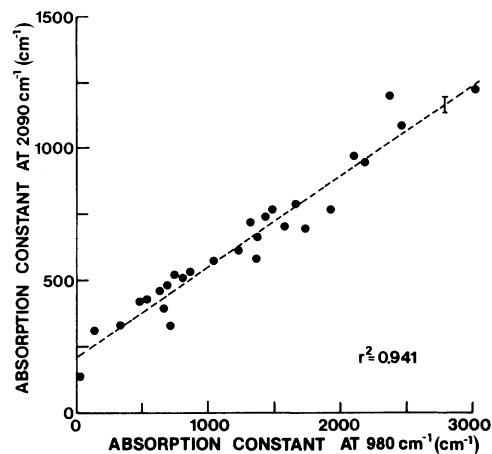


FIG. 5. Absorption constant at 2090 cm^{-1} vs absorption constant at 980 cm^{-1} . Dashed line is a linear regression analysis of the data. Error bars shown in the diagram and the r^2 value indicate the quality of the linear fit. The y -axis intercept represents absorption at 2090 cm^{-1} due to the SiH mode at 2000 cm^{-1} .

contrast the analysis of the 2090-cm^{-1} absorption yields a significantly larger offset on the y axis. This simply results from the fact that, in the absence of any oxygen in the films, and in samples with relatively low dihydride concentrations, the 2000-cm^{-1} SiH stretching vibration also produces some absorption at 2090 cm^{-1} . This is down from the peak value of absorption in the SiH band centered at 2000 cm^{-1} , but nevertheless is important in the analysis of the data discussed in this paper. Figures 2–5 then demonstrate that all four oxygen-related features scale with the oxygen concentration for the range we have studied, up to about 15 at. %.

Figure 6 indicates yet another interesting aspect of the alloy atom incorporation. We have plotted the integrated absorption in the Si–H bond-stretching regime ($\sim 2000\text{--}2100\text{ cm}^{-1}$) as a function of the integrated absorption in the Si–O–Si bond-stretching regime

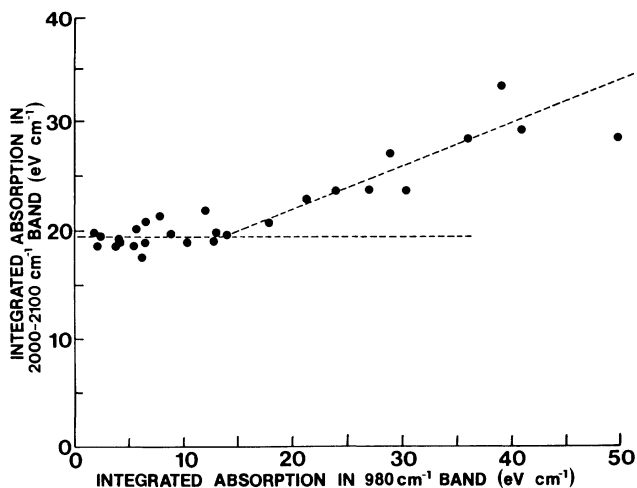


FIG. 6. Integrated absorption in the $(2000\text{--}2100)\text{-cm}^{-1}$ band vs integrated absorption in the 980-cm^{-1} band. Dashed lines indicate the trends in the data.

($\sim 900-1100\text{ cm}^{-1}$). For samples not containing oxygen, the integrated SiH bond-stretching absorption has been shown to be proportional to the concentration of bonded hydrogen.^{9,10} These films generally contain both monohydride and dihydride groups, so that direct comparison between these values and the values of integrated absorption in our films raises some questions. First of all our films do not contain dihydride groups as evidenced from the absence of sharp absorption bands between 800 and 900 cm^{-1} .^{9,12} Recall that isolated SiH_2 groups have a scissors mode at 875 cm^{-1} , while polymerized SiH_2 groups (SiH_2)_n have wagging and scissors modes at 845 and 890 cm^{-1} , respectively.^{12,13} Second, our films contain oxygen, which shifts the Si-H stretching band from 2000 to 2090 cm^{-1} and may also induce additional changes in the oscillator strength of the absorption. Returning then to Fig. 6, we have drawn two dashed lines to indicate trends in the data. For oxygen concentrations less than about 2 at. %, the hydrogen concentration, as measured by the integrated absorption, remains essentially unchanged. An integrated absorption of 20 eV cm^{-1} corresponds to a hydrogen concentration of approximately 15 at. %. For this same regime of oxygen concentrations, the absorption constant at 2090 cm^{-1} doubles relative to its value in an oxygen-free film indicating that a significant portion of the oxygen has a hydrogen atom for its second neighbor.⁶ For oxygen concentrations in excess of 2 at. %, the integrated absorption in the SiH stretching bands increases approximately linearly with the oxygen concentration. We have used SIMS to measure the hydrogen concentration in one of these films and find that the concentration correlates with that obtained from the integrated SiH stretching absorption. This leads us to conclude that the increased SiH bond-stretching absorption is not the result of an increased oscillator strength induced by near-neighbor oxygen atoms, but rather is the result of increased oxygen incorporation in the films.

So far we have only considered films in which the hydrogen is incorporated in the monohydride-bonding geometry. We have also grown films at lower substrate temperatures, 50 and 100°C as opposed to 300°C , to increase the hydrogen concentration as well as to promote

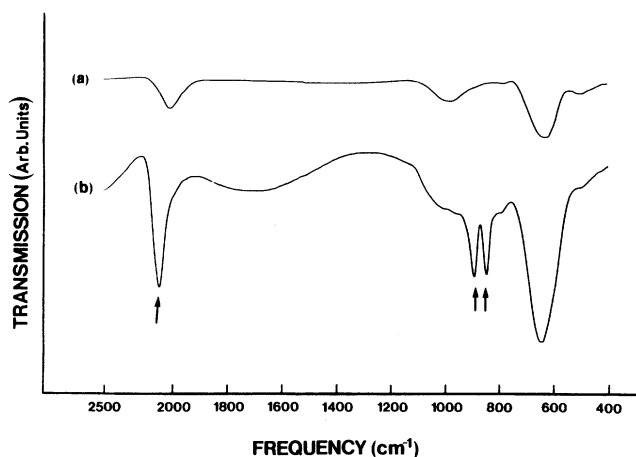


FIG. 7. Infrared absorption spectra of films produced with a substrate temperature of (a) 300°C and (b) 50°C . Arrows indicate the vibrations attributed to $(\text{SiH}_2)_n$ groups.

the formation of polymeric $(\text{SiH}_2)_n$.^{9,12} Figure 7 compares the spectra of a film produced at (a) a substrate temperature of 300°C with one produced at (b) a substrate temperature of 50°C . The arrows highlight the polysilane features; the sharpening and strengthening of the absorption band at 2100 cm^{-1} and the doublet with relatively sharp features at 890 and 845 cm^{-1} . The low-temperature film [Fig. 7(b)] does not display any additional oxygen-related features which could arise from the occurrence of oxygen atoms within the $(\text{SiH}_2)_n$ polymer chains, or from the occurrence of polymer chains terminated in a silicon atom which is bonded to an oxygen atom, except perhaps for some structure in the 980-cm^{-1} band. Each of these environments is expected to produce additional features in the 980-cm^{-1} band, as well as in the $(700-800)\text{-cm}^{-1}$ regime. Note that such features could be masked by the 780-cm^{-1} band already contributing to absorption in that same frequency range.

The low-temperature films have been shown to have a columnar structure and to be diphasic with the column material being alloyed *a*-Si containing hydrogen in the monohydride-bonding geometry, and the "connective" material being predominantly polysilane, $(\text{SiH}_2)_n$.¹⁴ The spectra discussed above are consistent with this description, provided that the column material is the *a*-Si:(H,O) alloy with bonding environments similar to the $T_s = 300^\circ\text{C}$ films, and with the connective material being $(\text{SiH}_2)_n$ with little or no oxygen "contamination."

Finally, Fig. 8(b) indicates the ir absorption in a film containing a significantly higher oxygen concentration, ~ 30 at. %. The upward-directed arrows highlight the oxygen-related features formed in films for which the concentration of oxygen is less than about 15 at. %. The downward-directed arrows indicate features associated with the increased oxygen concentration. A comparison between the integrated SiH vibrations in either the 2000 - or 630-cm^{-1} bands indicates that the hydrogen concentration in the two films shown in Figs. 8(a) and 8(b), respectively, are about the same and less than 20 at. %. This

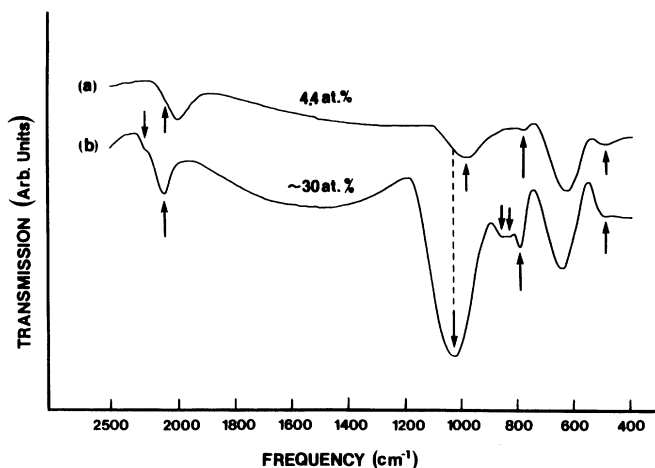


FIG. 8. Infrared absorption spectra of films with differing oxygen concentrations: (a) 4.4 at. % and (b) ~ 30 at. %. Upward-directed arrows are the vibrational modes associated with the local Si-O-Si-H bonding configurations. Downward-directed arrows represent absorptions that are associated with the increased oxygen content of the films.

means that the oxygen concentration in the film in Fig. 8(b) exceeds the hydrogen concentration in that film. We show in the next section that the features at 2250, 850, and 875 cm^{-1} are associated with both oxygen and hydrogen atoms, while the shift in the Si—O—Si stretching vibration from 980 to 1030 cm^{-1} is related simply to the increasing oxygen content. In $\alpha\text{-SiO}_2$, the Si—O—Si stretching band has its maximum absorption at 1080 cm^{-1} .¹¹

IV. DISCUSSION

We now discuss the experimental results in terms of the models discussed in Refs. 4 and 5. Consider first the ways in which hydrogen and oxygen can be incorporated into thin films of $\alpha\text{-Si}$. We restrict this discussion to the situation in which the hydrogen is incorporated in the monohydride or SiH configuration. Figure 9 indicates four relevant bonding arrangements: (a) and (b) are bonding geometries in which the hydrogen and oxygen atoms are not bonded to a common silicon site; (c) and (d) are two arrangements in which the oxygen and hydrogen atoms are bonded to a common silicon atom, and in which the Si—H bond is in the plane of the Si—O—Si bond. The vibrations of the "isolated" monohydride or SiH configuration in $\alpha\text{-Si}$ host are well known. They are a stretching motion in the direction of the Si—H bond, ν_S in Fig. 10(a), and a doubly degenerate bending mode, ν_B [also in Fig. 10(a)] with the hydrogen-atom motion perpendicular to the Si—H bond: $\nu_S \approx 2000 \text{ cm}^{-1}$ and $\nu_B \approx 630 \text{ cm}^{-1}$.¹² The isolated bridging oxygen site has three vibrations which are best described by considering the nature of the oxygen motion relative to the plane of the Si—O—Si bond, and, in particular, relative to the symmetry axis that is coincident with the bisector of the Si—O—Si bond angle. In Fig. 10(b), ν'_S is a stretching mode wherein the oxygen-atom motion is in the Si—O—Si bonding plane parallel to a line joining the two silicon atoms. ν'_B is also motion of the oxygen atom in the Si—O—Si bonding plane, but with the oxygen-atom displacement along the direction of the bisector of the Si—O—Si bond angle. Finally, ν'_R is an out-of-plane bond-rocking motion. Studies on $\alpha\text{-Si:O}$

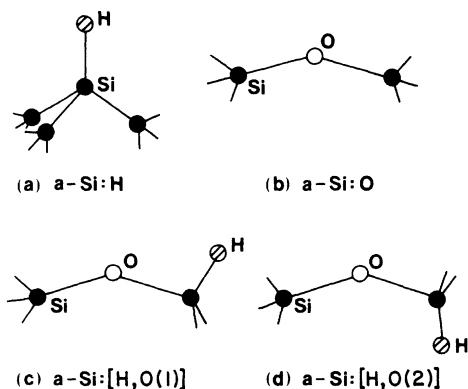


FIG. 9. Local bonding configurations: (a) The isolated Si—H group, (b) the isolated Si—O—Si group in $\alpha\text{-Si:O}$, and (c) and (d) local bonding arrangements in which the H and O atoms are bonded to the same Si site. In both (c) and (d) the Si—H bond is in the plane determined by the Si—O—Si group.

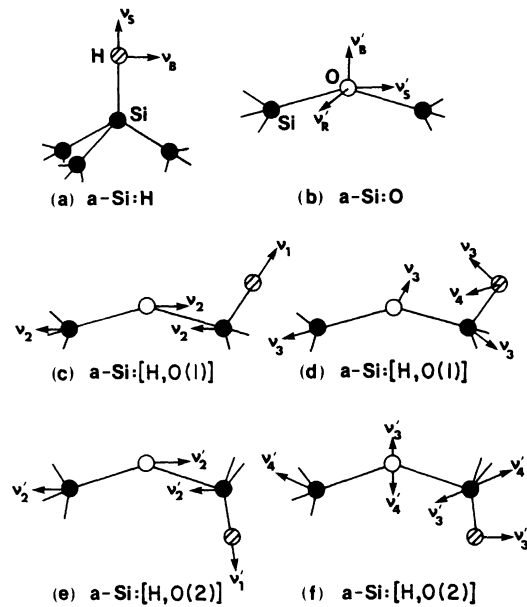


FIG. 10. Atomic displacements for localized vibrational modes: (a) The isolated Si—H group, (b) the isolated Si—O—Si group, (c) and (d) the Si—O—Si—H bonding configuration in Figs. 9(c), and (e) and (f) the Si—O—Si—H bonding configuration in Fig. 9(d).

layers produced via ion implantation have shown that $\nu'_S = 940$, $\nu'_B = 650$, and $\nu'_R = 500 \text{ cm}^{-1}$.⁷

Figure 1(a) indicates the absorption in a film with an oxygen concentration substantially less than the hydrogen concentration. The designations ν_1 , ν_2 , ν_3 , and ν_4 indicate the oxygen-related absorption bands. For reference the figure also includes the position of the ν_S and ν_B vibrations of the isolated SiH group and the positions of the ν'_S , ν'_B , and ν'_R of the isolated Si—O—Si group. The first observation that we make is that the four oxygen-related absorptions are not simply related to isolated Si—O—Si and/or SiH bonding configurations. This is evidenced by (1) the shifts of the SiH and Si—O—Si stretching vibrations, ν_S and ν'_S , respectively to higher frequencies (from 2000 to 2090 cm^{-1} for the first case and from 940 to 980 cm^{-1} for the second case), and (2) by the occurrence of a new absorption at 780 cm^{-1} . The four oxygen-related absorptions must then be interpreted in terms of bonding configurations in which the oxygen and hydrogen atoms are bonded to the *same* or nearby silicon sites. There is no evidence for ir absorption associated with OH groups.

The first evidence for the bonding of hydrogen and oxygen atoms to a common silicon atom derives from the presence of absorption at 2090 cm^{-1} that is not accompanied by absorption at either 875 cm^{-1} or a doublet at 890 and 845 cm^{-1} . The correlated absorption at 2090 and 875 cm^{-1} has been assigned to isolated SiH_2 groups^{12,13} and that at 2090, 890, and 845 cm^{-1} to polysilane or $(\text{SiH}_2)_n$ configurations.^{12,13} An analysis of chemical-bonding effects on the frequencies of SiH vibrations predicts that the presence of a strongly electronegative atom, such as oxygen, backbonded to one of the three positions available on the silicon atom of an SiH group would shift the SiH frequency to higher frequency. For

TABLE I. Comparison of the frequencies of the ir absorption bands with model calculations.

Experimental results (cm ⁻¹)			Model calculations (cm ⁻¹)			
<i>a</i> -Si:H ^a	<i>a</i> -Si:O ^b	<i>a</i> -Si:(H,O)	Si—H	Si—O—Si	Si—O—Si—H	
10 at. % H	5 at. % O	10 at. % H 3 at. % O			<i>trans</i>	<i>cis</i>
630	500	500	$\nu_B = 630$	$\nu'_R = 500$	$\nu'_1 = 2090$	$\nu_1 = 2090$
2000	650	630	$\nu_S = 2000$	$\nu'_B = 650$	$\nu'_2 = 980$	$\nu_2 = 980$
	940	780		$\nu'_S = 940$	$\nu'_3 = 650$	$\nu_3 = 750$
		980			$\nu'_4 = 630$	$\nu_4 = 630$
		2090				

^aReference 9 and 12.^bReference 7.

oxygen the predicted frequency shift is to ~ 2100 cm⁻¹.^{6,12} This then establishes the origin of the 2090-cm⁻¹ absorption displayed in all four of the samples shown in Fig. 1.

Consider next configurations involving both oxygen and hydrogen atoms being bonded to the same silicon site. These sites can be classified by the orientation of the SiH bond relative to the plane defined by the Si—O—Si bond. Of all of the possible configurations two are favored energetically. These are the configurations shown in Figs. 9(c) and 9(d). These arrangements minimize repulsive interaction between the nonbonding $2p$ electrons of the bridging oxygen atoms and the electrons contributing to the SiH bond. Note that the nonbonding p electrons of the oxygen atoms are oriented perpendicular to the plane of the Si—O—Si bond. Two different conformations are then possible: the *cis* conformation in Fig. 9(c) and the *trans* conformation in Fig. 9(d). The local-mode frequencies for these two bonding arrangements have been calculated and reported in Refs. 4 and 5. Table I summarizes the results of these calculations, which we now discuss with reference to the atomic motions illustrated in Figs. 10(c)—10(f).

The two bonding sites have two vibrations, designated in the figure as ν_1 and ν'_1 and ν_2 and ν'_2 , which do not depend on the nature of the particular bonding conformation. ν_1 and ν'_1 [Figs. 10(c) and 10(e), respectively] are bond-stretching vibrations of the SiH group. Since the mass of hydrogen is much less than that of silicon, these vibrations involve mostly hydrogen-atom motion. With the use of force constants that are derived from a chemical-bonding model, the calculated frequencies of 2090 cm⁻¹ are essentially the same as those determined from the ir absorption bands. ν_2 and ν'_2 in Figs. 10(c) and 10(e), respectively, are oxygen (asymmetric) stretching vibrations. Since the mass of oxygen is about equal to one-half that of silicon, these vibrations involve silicon and oxygen displacements of comparable magnitude. The calculated frequencies of 980 cm⁻¹ fall at the center of the broad absorption. The vibrations that are sensitive to the details of the bonding geometry; e.g., the *cis* or *trans* conformation of the oxygen and hydrogen atoms, are those vibrations involving a bending motion of the oxygen atom, i.e., oxygen-atom motion along the bisector of the Si—O—Si bond angle.

Consider first the *cis* conformation shown in Fig. 9(c) and the ν_3 vibration indicated in Fig. 10(d). The analysis presented in Refs. 4 and 5 indicates that ν_3 is a mode with

strongly coupled Si—H and Si—O—Si motions. The Si—H motion is predominantly a bending motion with the hydrogen-atom displacement perpendicular to the Si—H bond. The oxygen-atom motion is predominantly a bond-bending motion, but with a small admixture of stretching. The motion is therefore mostly in the direction of the bisector of the Si—O—Si bond, but also has a smaller component in the stretching direction, with the combined effect of an oxygen displacement that is displaced from the symmetry axis of the Si—O—Si group in the direction of the Si—H bond. ν_4 in Fig. 10(d) is simply an out-of-plane Si—H bending vibration. The calculated frequencies of ν_3 and ν_4 are 750 and 630 cm⁻¹, respectively. Consider next the *trans* configuration, Fig. 9(d), and the vibrations shown in Fig. 10(f). These are two vibrations which involve an oxygen bending motion. One of these, ν'_3 , is a coupled mode involving pure bending motions of both the oxygen and hydrogen atoms. The calculated frequency for this mode is 650 cm⁻¹. The second vibration ν'_4 is simply a pure oxygen bending mode with a calculated frequency of 630 cm⁻¹. We also find an out-of-plane hydrogen bending mode at 630 cm⁻¹ which is not shown in Fig. 10.

The spectra shown in Fig. 1 all display absorption at 780 cm⁻¹, which in turn scales linearly with the absorption at 980 cm⁻¹ (see Fig. 4). This means that a significant and constant fraction of the oxygen atoms go into a bonding environment similar to that shown in Fig. 9(c). There is no distinct feature associated with the *trans* conformation [Fig. 9(d)] so that it is impossible to estimate the ratio of oxygen and hydrogen atoms in these two configurations; however, the scaling illustrated in Fig. 4 indicates that this fraction is constant for the regime of oxygen incorporation we have studied.

As noted in Sec. III, the oxygen-related absorptions in films displaying dihydride as well as monohydride SiH vibrations show no additional oxygen-related features (see Fig. 7). This implies that oxygen atoms are not incorporated, at least in significant numbers, into the polysilane chains. Further evidence for this comes from the absence of oxygen-shifted SiH₂ stretching modes.⁶ Films of polysilane subjected to post oxidation display additional features at frequencies in excess of 2100 cm⁻¹ that can be interpreted as oxygen-shifted SiH₂ stretching vibrations.^{3,6}

Finally, the spectra of films with substantially higher oxygen concentrations have been shown to exhibit additional oxygen- and hydrogen-related features. These have been studied experimentally in some detail,² and are dis-

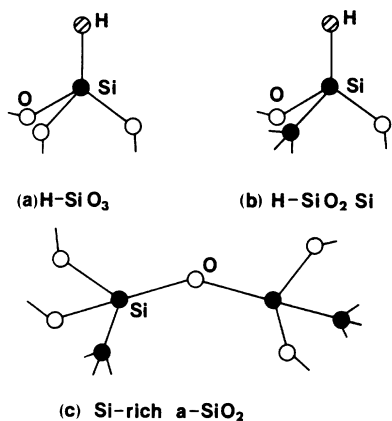


FIG. 11. Local bonding configurations for films containing high oxygen concentrations. In each instance, we show more than one oxygen bonded to a given silicon atom.

cussed in Ref. 4. The additional features indicated by the downward-directed arrows in Fig. 8(b) are then related to the bonding environments shown in Fig. 11. The Si—H stretching mode at 2250 cm^{-1} is associated with a bonding arrangement in which the silicon atom has three oxygen neighbors, as for example in Fig. 11(a) which shows a hydrogen atom substituting for an oxygen atom in $\alpha\text{-SiO}_2$.⁶ The bending mode of this configuration is at approximately 875 cm^{-1} . As expected, this vibration is also evident in our films. The absorption at 850 cm^{-1} is the bending motion of a Si—H bond in which the silicon atom has two oxygen neighbors and one silicon neighbor [see Fig. 11(b)]. The Si—H stretching mode of this group is at 2190 cm^{-1} and contributes to an unresolved feature in the spectrum in Fig. 8(b). Finally, the absorption at 1030 cm^{-1} is associated with the stretching mode of an Si—O—Si configuration, in which the silicon atoms are in turn bonded to other oxygen atoms. If we scale linearly from a frequency of 940 cm^{-1} for an isolated Si—O—Si group in an $\alpha\text{-Si}$ network to 1080 cm^{-1} for the Si—O—Si stretching vibration in $\alpha\text{-SiO}_2$, then the frequency of 1030 cm^{-1} means that approximately four of the six bonding positions of the two silicon atoms of the Si—O—Si configuration have bridging oxygen atoms attached to them [see Fig. 11(c)]. The remaining two positions have either Si or hydrogen neighbors. This estimate is consistent with the film composition, approximately 30 at. % of oxygen.

V. SUMMARY

We have produced alloys of $\alpha\text{-Si}:(\text{H},\text{O})$ by the glow-discharge decomposition of SiH_4 in a gas ambient containing both H_2 and O_2 , and studied the local bonding geometries of the H and O alloy atoms by ir absorption

spectroscopy. We find four oxygen-related absorptions, at 2090 , 980 , 780 , and 500 cm^{-1} , all of which are explained by local bonding arrangements in which both of the alloy atoms are bonded to the same Si site. The band at 780 cm^{-1} has been shown elsewhere^{4,5} to be a coupled mode involving both Si—H and Si—O—Si motions, and further to be associated with a bonding geometry in which the Si—H bond is coplanar with the Si—O—Si group, and in which the O and H atoms are in a *cis*-type bonding configuration. The linear scaling between the absorption constant at 780 cm^{-1} and the total oxygen-related absorption, as monitored by the 980-cm^{-1} band, establishes (1) that a significant fraction of the alloy atoms are in the *cis* bonding arrangement, and (2) that the fraction of atoms in this geometry is constant over the range of H and O concentrations we have studied.

Note added in proof. We have recently prepared films of $\alpha\text{-Si}:(\text{D},\text{O})$ by the glow-discharge decomposition of mixtures of SiD_4 and O_2 , and have studied their ir absorption spectra. The interpretation of these spectra as it relates to the local bonding environments of the O and D atoms fully supports the assignments and the structural model presented in this paper. In particular, the D-for-H substitution shifts all vibrations involving substantial H-atom motion to lower wave number. In addition, the substitution changes the nature of the 780-cm^{-1} coupled mode in alloy films grown with $T_s = 400^\circ\text{C}$. In the $\alpha\text{-Si}:(\text{H},\text{O})$ alloys, this mode derives from a coupling of a mixed bending-stretching O-atom motion with a H-atom bending, whereas in the $\alpha\text{-Si}:(\text{D},\text{O})$ alloys the “corresponding” vibration at 650 cm^{-1} involves pure bending motions of both the O and D atoms (see Fig. 3 of Ref. 4). We have also found evidence in low- T_s films for bonding configurations in which one O and two H atoms are bonded to the same Si atom. These are readily evident in the low- T_s films, but only with higher concentrations of bonded oxygen than for the film discussed in this paper. Additional evidence for this assignment has been obtained via the D-for-H atom substitution. For further details, refer to a paper by G. Lucovsky, S. S. Chao, J. Yang, J. Tyler, and W. Czubatyj [J. Vac. Sci. Technol. (in press)].

ACKNOWLEDGMENTS

We would like to thank L. Taylor, L. Contardi, G. DeMaggio, and A. Chan for their assistance in the preparation and measurements of the samples. We also thank D. Wickerhan for his art work. We gratefully acknowledge partial financial support from the Standard Oil Company, Company (Ohio) and the constant encouragement of S. R. Ovshinsky.

*Permanent address: Department of Physics, North Carolina State University, Raleigh, N.C. 27650.

¹M. A. Paesler, D. A. Anderson, E. C. Freeman, G. Moddell, and W. Paul, Phys. Rev. Lett. **41**, 1492 (1978).

²J. C. Knights, R. A. Street, and G. Lucovsky, J. Non-Cryst. Solids **35-36**, 279 (1980).

³P. John, I. M. Odeh, M. J. K. Thomas, M. J. Tricker, and J. I. B. Wilson, Phys. Status Solidi B **105**, 499 (1981).

⁴G. Lucovsky, Sol. Energy Mater. **8**, 165 (1982).

⁵G. Lucovsky and W. B. Pollard, J. Vac. Sci. Technol. A **1**, 313 (1983).

⁶G. Lucovsky, Solid State Commun. **29**, 571 (1979).

- ⁷G. Lucovsky, S. S. Chao, and R. Tsu (unpublished).
- ⁸J. C. Knights, in *Structure and Excitation of Amorphous Solids (Williamsburg, Virginia, 1976)*, Proceedings of an International Conference on Structure and Excitation of Amorphous Solids, edited by G. Lucovsky and F. L. Galeener (AIP, New York, 1976), p. 296.
- ⁹M. H. Brodsky, M. Cardona, and J. J. Cuomo, *Phys. Rev. B* **16**, 3556 (1977).
- ¹⁰H. Fritzsche, *Sol. Energy Mater.* **3**, 447 (1980).
- ¹¹F. L. Galeener and G. Lucovsky, in *Structure and Excitation of Amorphous Solids (Williamsburg, Virginia, 1976)*, Proceedings of an International Conference on Structure and Excitation of Amorphous Solids, edited by G. Lucovsky and F. L. Galeener (AIP, New York, 1976), p. 223.
- ¹²G. Lucovsky, R. J. Nemanich, and J. C. Knights, *Phys. Rev. B* **18**, 4288 (1978).
- ¹³W. B. Pollard and G. Lucovsky, *Phys. Rev. B* **26**, 3172 (1982).
- ¹⁴R. J. Nemanich, D. K. Biegelsen, and M. P. Rosenblum, *J. Phys. Soc. Jpn.* **49**, Suppl. A, 1189 (1980).